

ACHIEVING FULL-DIVERSITY AND FAST MAXIMUM LIKELIHOOD DECODING IN ASYNCHRONOUS ANALOG NETWORK CODING

Yun Liu^{*}, Wei Zhang[†], Soung Chang Liew[§] and P. C. Ching^{*}

^{*} Department of Electronic Engineering, The Chinese University of Hong Kong, Hong Kong, China

[†] School of Electrical Engineering & Telecommunications, The University of New South Wales, Australia

[§] Information Engineering Department, The Chinese University of Hong Kong, Hong Kong, China

Emails: yliu@ee.cuhk.edu.hk; wzhang@ee.unsw.edu.au; soung@ie.cuhk.edu.hk; pcching@ee.cuhk.edu.hk

ABSTRACT

This study designs space-time codes in analog network coding for asynchronous two-way relay networks, where asynchronous transmissions can cause diversity loss. We propose a novel code, called zero-padded interleave reversal Alamouti code (ZP-IR AC) to achieve full diversity with fast maximum likelihood decoding. Specifically, to combat symbol misalignment caused by asynchronous transmissions, the two terminals insert zero padding when transmitting to relays. Thereafter, the second relay performs an interleave reversal procedure to retain full diversity at each terminal. A salient feature of ZP-IR AC is that it can be decoupled into several independent parts that facilitate fast maximum likelihood decoding. Simulations of ZP-IR AC show full diversity gain. The bit error rate performance of ZP-IR AC is comparable to that of the synchronized Alamouti code and outperforms those of some recent schemes.

Index Terms— Analog network coding, asynchronous, space-time codes, full diversity, maximum likelihood decoding.

1. INTRODUCTION

Analog network coding (ANC) [1] is an efficient strategy to double the bandwidth efficiency of two-way relay networks, where two terminals simultaneously exchange information with the assist of relays. A typical ANC scheme includes two phases. In Phase I, the two terminals send signals to the relays simultaneously. The relays process the received superimposed signals and broadcast them in Phase II. Each terminal subtracts the self-interference signal and obtains the signal from the other terminal. The benefits of multiple relays was further investigated in [2–5]. By establishing cooperation among relays, space-time codes (STC) are used to achieve diversity gain in this network.

Asynchronous transmission, an issue that arises from relay networks, has attracted much attention [6–10]. Given the distributed nature of relay networks, the path delays from different relays to terminals are generally different. The lack of perfect synchronization causes symbol misalignment, which can cause severe performance degradation [8, 9]. Symbol misalignment in two-way relay networks comes in two types. The first type occurs in Phase I when simultaneous but asynchronous transmissions from terminals to each relay lead to symbol misalignment at the relays. Note that this type only occurs in two-way relay networks and never in one-way relay networks. The second type occurs in Phase II when asynchronous transmissions from relays to each terminal lead to symbol misalignment at the terminals, thus resulting in diversity loss in STCs [7, 9]. Intensive studies on asynchronous STC [9, 11–21] have been proposed to

tackle the second type. However, the existence of the first type has rendered these studies on one-way relay networks not applicable to two-way relay networks. Therefore, several schemes have reconsidered the asynchronous issue in two-way relay networks [22–24].

These schemes can be categorized as either frequency domain approaches or time domain approaches. For frequency domain approaches, the authors in [22, 23] considered frequency selective fading channel and adopted orthogonal frequency division multiplexing (OFDM), where cyclic prefix (CP) was applied to combat symbol misalignment. Thus, such approaches may not be applicable for non-OFDM systems. Besides, OFDM also has its own drawbacks like code rate loss due to CP or carrier frequency offsets (CFO).

This study is related to prior works in time domain approaches. With the goal of avoiding such drawbacks of OFDM, the authors in [24] proposed a time domain approach to achieve full diversity. By using shift-full-rank matrix [12, 25], the approach in [24] successfully achieves full diversity. Unfortunately, the maximum likelihood (ML) decoding of this time domain approach is prohibitively complex. The authors resorted to linear decoders for simplicity at the expense of degraded error-rate performance.

This study proposes a zero-padded interleave reversal Alamouti code (ZP-IR AC) in a two-way relay network with two single-antenna relays. In Phase I, terminals transmit with zero padding to combat symbol misalignment at the relay. Then the second relay performs an interleave reversal procedure, and both relays broadcast the signals back to terminals at Phase II. We prove that full diversity gain is achieved in this scheme. Moreover, ZP-IR AC is amenable to fast ML decoding since its code structure can be decoupled. Simulation results show the full diversity gain in ZP-IR AC.

Notation: Vector $\mathbf{x}[i:j]$ represents a sub-vector in \mathbf{x} from index i to index j . Note that we allow $j < i$. If $i < j$, $\mathbf{x}[i:j] = [\mathbf{x}[i], \mathbf{x}[i+1], \dots, \mathbf{x}[j]]$; if $i > j$, $\mathbf{x}[i:j] = [\mathbf{x}[i], \mathbf{x}[i-1], \dots, \mathbf{x}[j]]$. $\mathbf{x}^*[i]$ represents the conjugate signal of $\mathbf{x}[i]$.

2. PROBLEM FORMULATION

2.1. System Model

We consider a two-way relay network with two single-antenna relays assisting the information exchange between two single-antenna terminals A and B as shown in Fig. 1. Each node works in half-duplex mode. In Phase I, the channel fading coefficient from J to R_i is $h_{i,J}$, and in Phase II, the channel fading coefficient from R_i to J is $\hat{h}_{i,J}$, $i = 1, 2$, $J = A, B$. In Phase I, $h_{i,J}$ is only known at R_i . In Phase II, $\hat{h}_{i,J}$ is known at terminal J , and all channel fading coefficients in Phase I are also known at terminal J . The path delay between R_i

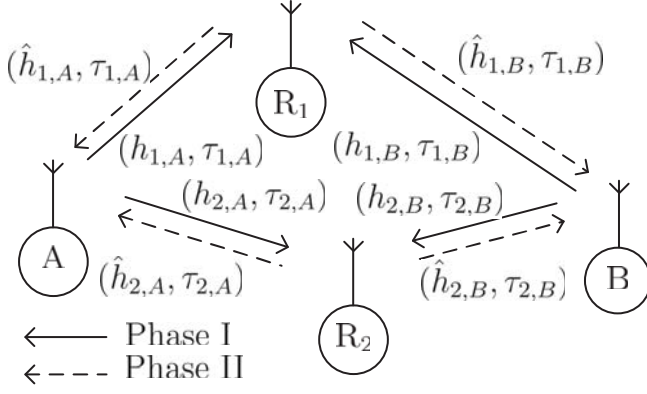


Fig. 1: An asynchronous two-way relay network with two single-antenna relays

and J is $\tau_{i,J}$, $i = 1, 2$, $J = A, B$. For simplicity, $\tau_{i,J}$ is assumed to be an integer multiple of the symbol duration. The fractional part of $\tau_{i,J}$ can be regarded as multipath effects to be addressed by equalizers [11]. In Phase I, R_i knows $\tau_{i,A}$ and $\tau_{i,B}$, and in Phase II, terminals know all delay coefficients. The delay difference bound is denoted by τ_m , where $|\tau_{i,J} - \tau_{\hat{i},\hat{J}}| \leq \tau_m$, $[i, J] \neq [\hat{i}, \hat{J}]$, for $i, \hat{i} \in \{1, 2\}$, $J, \hat{J} \in \{A, B\}$. τ_m is known at all nodes.

Considering the multiple transmissions in these two phases, a proper power allocation strategy is critical for high power efficiency. According to [26], the adopted power allocation is

$$P_A = P_B = P_r = \frac{P}{4}, \quad (1)$$

where P_A and P_B denote the transmit power of A and B , respectively. The transmit power of each relay antenna is P_r , and the overall power, namely the sum of all transmit power, is P . To ensure (1), R_i amplifies the received signal with α_i , $i = 1, 2$.

$$\alpha_i = \frac{1}{\sqrt{\frac{P}{4}|h_{i,A}|^2 + \frac{P}{4}|h_{i,B}|^2 + 1}}$$

2.2. Diversity Loss Problem

In ANC, the asynchronous transmissions in Phase I lead to symbol misalignment at relays. This condition may further cause diversity loss in Phase II. To elucidate this problem, we provide an example of bounded delay-tolerant time interleave reversal Alamouti codes (BDT-TIR AC) [21]. The structure of BDT-TIR AC is shown in C.

$$\mathbf{C} = \begin{bmatrix} \mathbf{c}[1] & \mathbf{c}[2] & \mathbf{c}[3] & \mathbf{c}[4] \\ -\mathbf{c}^*[3] & -\mathbf{c}^*[4] & \mathbf{c}^*[1] & \mathbf{c}^*[2] \end{bmatrix} \quad (2)$$

BDT-TIR AC achieves full diversity in one-way relay networks, but it is not applicable to two-way relay networks.

Example 1: Let us consider the network in Fig. 1. The path delay coefficients $[\tau_{1,A}, \tau_{1,B}, \tau_{2,A}, \tau_{2,B}] = [1, 1, 1, 0]$. Two symbol sequences $\mathbf{a} = [\mathbf{a}[1], \mathbf{a}[2], \mathbf{a}[3], \mathbf{a}[4]]$ and $\mathbf{b} = [\mathbf{b}[1], \mathbf{b}[2], \mathbf{b}[3], \mathbf{b}[4]]$ are exchanged between terminals A and B .

• In Phase I, terminal A transmits \mathbf{a} , and terminal B transmits \mathbf{b} . The received signal vectors at R_1 and R_2 are

$$\begin{aligned} \mathbf{y}_{R_1} &= \sqrt{\frac{P}{4}} [h_{1,A}, h_{1,B}] \begin{bmatrix} 0 & \mathbf{a}[1] & \mathbf{a}[2] & \mathbf{a}[3] & \mathbf{a}[4] \\ 0 & \mathbf{b}[1] & \mathbf{b}[2] & \mathbf{b}[3] & \mathbf{b}[4] \end{bmatrix} + \mathbf{n}_1, \\ \mathbf{y}_{R_2} &= [\mathbf{y}_{R_2}[1], \mathbf{y}_{R_2}[2], \mathbf{y}_{R_2}[3], \mathbf{y}_{R_2}[4], \mathbf{y}_{R_2}[5]] \\ &= \sqrt{\frac{P}{4}} [h_{2,A}, h_{2,B}] \begin{bmatrix} 0 & \mathbf{a}[1] & \mathbf{a}[2] & \mathbf{a}[3] & \mathbf{a}[4] \\ \mathbf{b}[1] & \mathbf{b}[2] & \mathbf{b}[3] & \mathbf{b}[4] & 0 \end{bmatrix} + \mathbf{n}_2. \end{aligned}$$

R_1 transforms \mathbf{y}_{R_1} into $\hat{\mathbf{y}}_{R_1}$, given by

$$\hat{\mathbf{y}}_{R_1} = \mathbf{y}_{R_1}[2:5] = \sqrt{\frac{P}{4}} [h_{1,A}, h_{1,B}] \underbrace{\begin{bmatrix} \mathbf{a}[1] & \mathbf{a}[2] & \mathbf{a}[3] & \mathbf{a}[4] \\ \mathbf{b}[1] & \mathbf{b}[2] & \mathbf{b}[3] & \mathbf{b}[4] \end{bmatrix}}_{\mathbf{x}_{R_1}} + \hat{\mathbf{n}}_1. \quad (3)$$

The asynchronous transmissions in Phase I lead to symbol misalignment in \mathbf{y}_{R_2} . Due to symbol misalignment, R_2 reconstructs $\hat{\mathbf{y}}_{R_2}$ as

$$\begin{aligned} \hat{\mathbf{y}}_{R_2} &= [\mathbf{y}_{R_2}^*[1], -\mathbf{y}_{R_2}^*[4], -\mathbf{y}_{R_2}^*[5], \mathbf{y}_{R_2}^*[2], \mathbf{y}_{R_2}^*[3]] \\ &= \sqrt{\frac{P}{4}} [h_{2,A}^*, h_{2,B}^*] \underbrace{\begin{bmatrix} 0 & -\mathbf{a}^*[3] & -\mathbf{a}^*[4] & \mathbf{a}^*[1] & \mathbf{a}^*[2] \\ \mathbf{b}^*[1] & -\mathbf{b}^*[4] & 0 & \mathbf{b}^*[2] & \mathbf{b}^*[3] \end{bmatrix}}_{\mathbf{x}_{R_2}} + \hat{\mathbf{n}}_2. \end{aligned} \quad (4)$$

• In Phase II, the transmitted signals from R_1 and R_2 are $\alpha_1 \hat{\mathbf{y}}_{R_1}$ and $\alpha_2 \hat{\mathbf{y}}_{R_2}$, respectively.

After each terminal cancels the self-interference, the received signal vector becomes

$$\begin{aligned} \mathbf{y}_B &= \sqrt{\frac{P}{4}} [\alpha_1 h_{1,A} \hat{h}_{1,B}, \alpha_2 h_{2,A}^* \hat{h}_{2,B}] \\ &\underbrace{\begin{bmatrix} 0 & \mathbf{a}[1] & \mathbf{a}[2] & \mathbf{a}[3] & \mathbf{a}[4] \\ 0 & -\mathbf{a}^*[3] & -\mathbf{a}^*[4] & \mathbf{a}^*[1] & \mathbf{a}^*[2] \end{bmatrix}}_{\mathbf{x}_a} + \hat{\mathbf{n}}_B. \\ \mathbf{y}_A &= \sqrt{\frac{P}{4}} [\alpha_1 \hat{h}_{1,A} h_{1,B}, \alpha_2 \hat{h}_{2,A} h_{2,B}^*] \\ &\underbrace{\begin{bmatrix} 0 & \mathbf{b}[1] & \mathbf{b}[2] & \mathbf{b}[3] & \mathbf{b}[4] & 0 \\ 0 & \mathbf{b}^*[1] & -\mathbf{b}^*[4] & 0 & \mathbf{b}^*[2] & \mathbf{b}^*[3] \end{bmatrix}}_{\mathbf{x}_b} + \hat{\mathbf{n}}_A. \end{aligned}$$

The last four columns of \mathbf{X}_a has the same structure as \mathbf{C} , thereby guaranteeing full diversity on \mathbf{a} . However, \mathbf{X}_b no longer follows \mathbf{C} . The difference matrix of \mathbf{X}_b is

$$\Delta \mathbf{X}_b = \begin{bmatrix} 0 & \Delta \mathbf{b}[1] & \Delta \mathbf{b}[2] & \Delta \mathbf{b}[3] & \Delta \mathbf{b}[4] & 0 \\ 0 & \Delta \mathbf{b}^*[1] & -\Delta \mathbf{b}^*[4] & 0 & \Delta \mathbf{b}^*[2] & \Delta \mathbf{b}^*[3] \end{bmatrix}.$$

When $\Delta \mathbf{b}[1] \neq 0$ and $\Delta \mathbf{b}[2] = \Delta \mathbf{b}[3] = \Delta \mathbf{b}[4] = 0$, $\Delta \mathbf{X}_b$ is only of rank one, which indicates diversity loss.

We summarize the reasons of diversity loss as follows: 1) BDT-TIR AC requires clear separation of those four symbols into four parts; 2) Due to the asynchronous transmission in Phase I, the received signals at R_2 do not have such separation, rendering unqualified structure in \mathbf{X}_{R_2} , which results in diversity loss.

3. NEW CODE DESIGN

This section presents ZP-IR AC to overcome the diversity loss due to symbol misalignment. The basic idea is to add zero padding to accommodate the symbol misalignment and maintain clear separation to fulfill the full-diversity code structure.

3.1. Code Structure

Terminal A transmits a sequence \mathbf{a} of $4l$ symbols, and terminal B transmits a sequence \mathbf{b} of $4l$ symbols, where $l \geq 2\tau_m$. For example, when $\tau_m = 1$, $4l \geq 8$, meaning that each sequence should contain at least 8 symbols. Later we will show that our code structure favors large l because of high code rate.

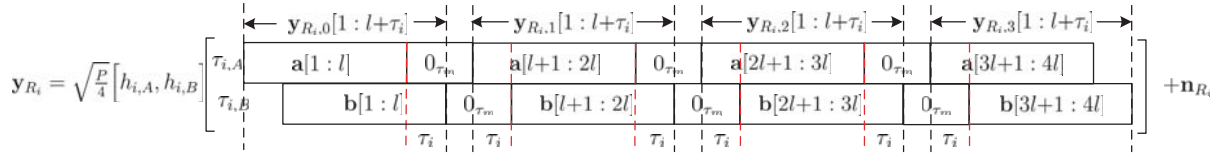


Fig. 2: Signal structure of \mathbf{y}_{R_i} , which is separated into $\mathbf{y}_{R_i,0}, \mathbf{y}_{R_i,1}, \mathbf{y}_{R_i,2}, \mathbf{y}_{R_i,3}$

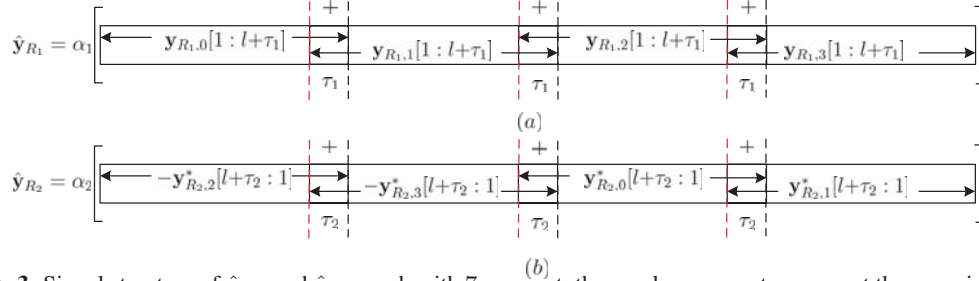


Fig. 3: Signal structure of $\hat{\mathbf{y}}_{R_1}$ and $\hat{\mathbf{y}}_{R_2}$, each with 7 segment; the overlap segments represent the sum signals

• In Phase I, terminals form groups of l symbols each, and insert a all-zero row vector with τ_m elements, $\mathbf{0}_{\tau_m}$, between each group, to construct $\hat{\mathbf{a}}$ and $\hat{\mathbf{b}}$:

$$\hat{\mathbf{a}} = [\mathbf{a}[1:l], \mathbf{0}_{\tau_m}, \mathbf{a}[l+1:2l], \mathbf{0}_{\tau_m}, \mathbf{a}[2l+1:3l], \mathbf{0}_{\tau_m}, \mathbf{a}[3l+1:4l]];$$

$$\hat{\mathbf{b}} = [\mathbf{b}[1:l], \mathbf{0}_{\tau_m}, \mathbf{b}[l+1:2l], \mathbf{0}_{\tau_m}, \mathbf{b}[2l+1:3l], \mathbf{0}_{\tau_m}, \mathbf{b}[3l+1:4l]].$$

The zero-padding is utilized to accommodate the symbol misalignment at relays, so as to maintain clear separation of four parts. The signal vector received by R_i is

$$\mathbf{y}_{R_i} = \sqrt{\frac{P}{4}} [h_{i,A}, h_{i,B}] \begin{bmatrix} \mathbf{0}_{\tau_{i,A}} & \hat{\mathbf{a}} & \mathbf{0}_{\hat{\tau}_{i,A}} \\ \mathbf{0}_{\tau_{i,B}} & \hat{\mathbf{b}} & \mathbf{0}_{\hat{\tau}_{i,B}} \end{bmatrix} + \mathbf{n}_{R_i}, \quad (5)$$

where $\hat{\tau}_{i,A} \triangleq \max\{\tau_{i,A}, \tau_{i,B} - \tau_{i,A}, 0\}$, and $\hat{\tau}_{i,B} \triangleq \max\{\tau_{i,A} - \tau_{i,B}, 0\}$, $i = 1, 2$. \mathbf{y}_{R_i} is separated into four parts as

$$\mathbf{y}_{R_i,j}[1:l+\tau_i]$$

$$= \mathbf{y}_{R_i} \left[\min\{\tau_{i,A}, \tau_{i,B}\} + j + \tau_m + 1 : \max\{\tau_{i,A}, \tau_{i,B}\} + (j+1)l + j\tau_m \right], \quad (6)$$

where $j = 0, 1, 2, 3$, and $\tau_i = |\tau_{i,A} - \tau_{i,B}|$, $i = 1, 2$.

$\mathbf{y}_{R_i,1}, \mathbf{y}_{R_i,2}, \mathbf{y}_{R_i,3}$ and $\mathbf{y}_{R_i,4}$ correspond to those four parts. Fig. 2 illustrates the separation.

The transmitted signals by R_1 , $\hat{\mathbf{y}}_{R_1}$ in Fig. 3 (a), contain 7 segments, corresponding to the 7 terms in (7).

$$\hat{\mathbf{y}}_{R_1} = \alpha_1 [\mathbf{y}_{R_1,0}[1:l], \mathbf{y}_{R_1,0}[l+1:l+\tau_1] + \mathbf{y}_{R_1,1}[1:\tau_1],$$

$$\mathbf{y}_{R_1,1}[\tau_1+1:l], \mathbf{y}_{R_1,1}[l+1:l+\tau_1] + \mathbf{y}_{R_1,2}[1:\tau_1], \mathbf{y}_{R_1,2}[\tau_1+1:l],$$

$$\mathbf{y}_{R_1,2}[l+1:l+\tau_1] + \mathbf{y}_{R_1,3}[1:\tau_1], \mathbf{y}_{R_1,3}[\tau_1+1:l+\tau_1]] \quad (7)$$

$$= \alpha_1 \sqrt{\frac{P}{4}} [h_{1,A}, h_{1,B}] \underbrace{\begin{bmatrix} \mathbf{0}_{\hat{\tau}_{1,B}} & \mathbf{a}[1:4l] & \mathbf{0}_{\hat{\tau}_{1,A}} \\ \mathbf{0}_{\hat{\tau}_{1,A}} & \mathbf{b}[1:4l] & \mathbf{0}_{\hat{\tau}_{1,B}} \end{bmatrix}}_{\mathbf{X}_1} + \hat{\mathbf{n}}_{R_1}.$$

If $\tau_1 = 0$, the underlined terms are removed from $\hat{\mathbf{y}}_{R_1}$.

The transmitted signals by R_2 , $\hat{\mathbf{y}}_{R_2}$ in Fig. 3 (b), contain 7 segments, corresponding to the 7 terms in (8).

$$\hat{\mathbf{y}}_{R_2} = \alpha_2 [-\mathbf{y}_{R_2,2}^*[l+\tau_2:\tau_2+1], -\mathbf{y}_{R_2,2}^*[\tau_2:1] - \mathbf{y}_{R_2,3}^*[l+\tau_2:l+1],$$

$$-\mathbf{y}_{R_2,3}^*[l:\tau_2+1], -\mathbf{y}_{R_2,3}^*[\tau_2:1] + \mathbf{y}_{R_2,0}^*[l+\tau_2:l+1], \mathbf{y}_{R_2,0}^*[l:\tau_2+1],$$

$$\mathbf{y}_{R_2,0}^*[\tau_2:1] + \mathbf{y}_{R_2,1}^*[l+\tau_2:l+1], \mathbf{y}_{R_2,1}^*[l:1]] \quad (8)$$

$$= \hat{\mathbf{n}}_2 + \alpha_2 \sqrt{\frac{P}{4}} [h_{2,A}^*, h_{2,B}^*]$$

$$\underbrace{\begin{bmatrix} \mathbf{0}_{\hat{\tau}_{2,B}} & -\mathbf{a}^*[3l:2l+1] & -\mathbf{a}^*[4l:3l+1] & \mathbf{a}^*[l:1] & \mathbf{a}^*[2l:l+1] & \mathbf{0}_{\hat{\tau}_{2,A}} \\ \mathbf{0}_{\hat{\tau}_{2,A}} & -\mathbf{b}^*[3l:2l+1] & -\mathbf{b}^*[4l:3l+1] & \mathbf{b}^*[l:1] & \mathbf{b}^*[2l:l+1] & \mathbf{0}_{\hat{\tau}_{2,B}} \end{bmatrix}}_{\mathbf{X}_2}.$$

If $\tau_2 = 0$, the underlined terms are removed from $\hat{\mathbf{y}}_{R_2}$.

By using zero padding, \mathbf{X}_1 and \mathbf{X}_2 keep the structure of \mathbf{C} in (2) on both \mathbf{a} and \mathbf{b} .

• In Phase II, R_1 transmits $\hat{\mathbf{y}}_{R_1}$ and R_2 transmits $\hat{\mathbf{y}}_{R_2}$. At terminal A , after canceling the self-interference on \mathbf{a} , the received signal vector is

$$\mathbf{y}_A = \hat{\mathbf{n}}_A + [\alpha_1 \hat{h}_{1,A} h_{1,B} + \alpha_2 \hat{h}_{2,A} h_{2,B}^*] \begin{bmatrix} \mathbf{0}_{\max\{\tau_{1,B}, \tau_{1,A}\}} \\ \mathbf{0}_{\max\{2\tau_{2,A} - \tau_{2,B}, \tau_{2,A}\}} \end{bmatrix}$$

$$\begin{bmatrix} \mathbf{b}[1:l] & \mathbf{b}[l+1:2l] & \mathbf{b}[2l+1:3l] & \mathbf{b}[3l+1:4l] & \mathbf{0}_{\max\{\tau_{A,0}\}} \\ -\mathbf{b}^*[3l:2l+1] & -\mathbf{b}^*[4l:3l+1] & \mathbf{b}^*[l:1] & \mathbf{b}^*[2l:l+1] & \mathbf{0}_{\max\{-\tau_{A,0}\}} \end{bmatrix}, \quad (9)$$

where $\tau_A \triangleq \max\{2\tau_{2,A} - \tau_{2,B}, \tau_{2,A}\} - \max\{\tau_{1,B}, \tau_{1,A}\}$.

\mathbf{y}_A in (9) can be further decoupled into $2(l - |\tau_A|)$ Alamouti code matrices and $|\tau_A|$ of 4-symbol matrices for fast decoding. The code structure of \mathbf{a} at B can be similarly derived.

Next, we use Example 2 to elucidate the code structure.

Example 2: Suppose $\tau_m = 1$, $4l = 8$, that is, $l = 2$, $P = 4$, and $[\tau_{1,A}, \tau_{1,B}, \tau_{2,A}, \tau_{2,B}] = [1, 1, 1, 0]$. $\tau_1 = |\tau_{1,A} - \tau_{1,B}| = 0$, and $\tau_2 = |\tau_{2,A} - \tau_{2,B}| = 1$. For simplicity, let $\alpha_1 = \alpha_2 = 1$.

According to (5), the received signal vectors at the relays are

$$\mathbf{y}_{R_1} = [h_{1,A}, h_{1,B}] \begin{bmatrix} 0 & \mathbf{a}[1] & \mathbf{a}[2] & 0 & \mathbf{a}[3] & \mathbf{a}[4] & 0 & \mathbf{a}[5] \\ 0 & \mathbf{b}[1] & \mathbf{b}[2] & 0 & \mathbf{b}[3] & \mathbf{b}[4] & 0 & \mathbf{b}[5] \\ \mathbf{a}[6] & 0 & \mathbf{a}[7] & \mathbf{a}[8] & & & & \\ \mathbf{b}[6] & 0 & \mathbf{b}[7] & \mathbf{b}[8] & & & & \end{bmatrix} + \mathbf{n}_1,$$

$$\mathbf{y}_{R_2} = [h_{2,A}, h_{2,B}] \begin{bmatrix} 0 & \mathbf{a}[1] & \mathbf{a}[2] & 0 & \mathbf{a}[3] & \mathbf{a}[4] & 0 & \mathbf{a}[5] \\ \mathbf{b}[1] & \mathbf{b}[2] & 0 & \mathbf{b}[3] & \mathbf{b}[4] & 0 & \mathbf{b}[5] & \mathbf{b}[6] \\ \mathbf{a}[6] & 0 & \mathbf{a}[7] & \mathbf{a}[8] & & & & \\ 0 & \mathbf{b}[7] & \mathbf{b}[8] & 0 & & & & \end{bmatrix} + \mathbf{n}_2.$$

According to (6), $\mathbf{y}_{R_1,0}[1:2] = \mathbf{y}_{R_1}[2:3]$, $\mathbf{y}_{R_1,1}[1:2] = \mathbf{y}_{R_1}[5:6]$, $\mathbf{y}_{R_1,2}[1:2] = \mathbf{y}_{R_1}[8:9]$ and $\mathbf{y}_{R_1,3}[1:2] = \mathbf{y}_{R_1}[11:12]$. Using (7), $\hat{\mathbf{y}}_{R_1}$ is

$$\hat{\mathbf{y}}_{R_1} = [\mathbf{y}_{R_1,0}[1:2], \mathbf{y}_{R_1,1}[1:2], \mathbf{y}_{R_1,2}[1:2], \mathbf{y}_{R_1,3}[1:2]]$$

$$= [h_{1,A}, h_{1,B}] \begin{bmatrix} \mathbf{a}[1] & \mathbf{a}[2] & \mathbf{a}[3] & \mathbf{a}[4] & \mathbf{a}[5] & \mathbf{a}[6] & \mathbf{a}[7] & \mathbf{a}[8] \\ \mathbf{b}[1] & \mathbf{b}[2] & \mathbf{b}[3] & \mathbf{b}[4] & \mathbf{b}[5] & \mathbf{b}[6] & \mathbf{b}[7] & \mathbf{b}[8] \end{bmatrix} + \hat{\mathbf{n}}_1.$$

According to (6), $\mathbf{y}_{R_2,0}[1:3] = \mathbf{y}_{R_2}[1:3]$, $\mathbf{y}_{R_2,1}[1:3] = \mathbf{y}_{R_2}[4:6]$, $\mathbf{y}_{R_2,2}[1:3] = \mathbf{y}_{R_2}[7:9]$ and $\mathbf{y}_{R_2,3}[1:3] = \mathbf{y}_{R_2}[10:12]$. Using (8), $\hat{\mathbf{y}}_{R_2}$ can be written as

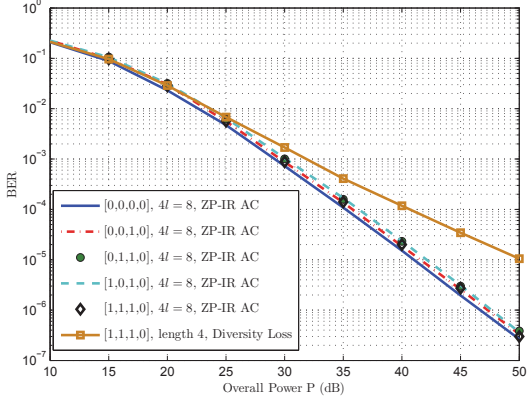


Fig. 4: BER performance of ZP-IR AC

$$\begin{aligned} \hat{\mathbf{y}}_{R_2} = & \left[-\mathbf{y}_{R_2,2}^*[3:2], -\mathbf{y}_{R_2,2}^*[1] - \mathbf{y}_{R_2,3}^*[3], -\mathbf{y}_{R_2,3}^*[2], -\mathbf{y}_{R_2,3}^*[1] + \right. \\ & \left. \mathbf{y}_{R_2,0}^*[3], \mathbf{y}_{R_2,0}^*[2], \mathbf{y}_{R_2,0}^*[1] + \mathbf{y}_{R_2,1}^*[3], \mathbf{y}_{R_2,1}^*[2:1] \right] \quad (10) \\ = & [\hat{h}_{2,A}^*, \hat{h}_{2,B}^*] \begin{bmatrix} -\mathbf{a}^*[6] & -\mathbf{a}^*[5] & -\mathbf{a}^*[8] & -\mathbf{a}^*[7] & \mathbf{a}^*[2] \\ 0 & -\mathbf{b}^*[6] & -\mathbf{b}^*[5] & -\mathbf{b}^*[8] & -\mathbf{b}^*[7] \\ \mathbf{a}^*[1] & \mathbf{a}^*[4] & \mathbf{a}^*[3] & 0 & \\ \mathbf{b}^*[2] & \mathbf{b}^*[1] & \mathbf{b}^*[4] & \mathbf{b}^*[3] & \end{bmatrix} + \hat{\mathbf{n}}_2. \end{aligned}$$

In Phase II, R_1 transmits $\hat{\mathbf{y}}_{R_1}$ and R_2 transmits $\hat{\mathbf{y}}_{R_2}$, simultaneously. At terminal A, \mathbf{y}_A in (9) becomes

$$\begin{aligned} \mathbf{y}_A = & [\hat{h}_{1,A} h_{1,B}, \hat{h}_{2,A} h_{2,B}^*] \begin{bmatrix} 0 & \mathbf{b}[1] & \mathbf{b}[2] & \mathbf{b}[3] & \mathbf{b}[4] & \mathbf{b}[5] \\ 0 & 0 & -\mathbf{b}^*[6] & -\mathbf{b}^*[5] & -\mathbf{b}^*[8] & -\mathbf{b}^*[7] \\ \mathbf{b}[6] & \mathbf{b}[7] & \mathbf{b}[8] & 0 & \\ \mathbf{b}^*[2] & \mathbf{b}^*[1] & \mathbf{b}^*[4] & \mathbf{b}^*[3] & \end{bmatrix} + \hat{\mathbf{n}}_A, \quad (11) \end{aligned}$$

From (11), we can detect the Alamouti code matrices on $(\mathbf{b}[2], \mathbf{b}[6])$ and $(\mathbf{b}[4], \mathbf{b}[8])$, and a 4-symbol matrix with $(\mathbf{b}[1], \mathbf{b}[3], \mathbf{b}[5], \mathbf{b}[7])$, which is discussed in [21]. Because of the decoupling nature, ZP-IR AC can be decoded with a fast ML decoder.

3.2. Full Diversity Proof

Theorem 1. Consider a system with two single-antenna relays, where the path delay difference is bounded by τ_m . Terminal A transmits a sequence \mathbf{a} with $4l$ symbols ($l \geq 2\tau_m$), and terminal B transmits a sequence \mathbf{b} with $4l$ symbols. ZP-IR AC achieves full diversity on both \mathbf{a} and \mathbf{b} .

Proof: From \mathbf{y}_A in (9), we can observe the structure of BDT-TIR AC. For BDT-TIR AC, full diversity is achieved provided that the path delay difference is smaller than l [21].

The delay difference between the two paths is

$$\left| \max\{\tau_{1,B}, \tau_{1,A}\} - \max\{2\tau_{2,A} - \tau_{2,B}, \tau_{2,A}\} \right| \leq 2\tau_m \leq l.$$

The same analysis can be applied to the code structure of \mathbf{a} at B. Therefore, full diversity is guaranteed. \square

3.3. Code Rate Analysis

The worst-case code rate R of ZP-IR AC is

$$R = \frac{4l + 4l}{8l + 6\tau_m + 2 \min\{\tau_{1,A}, \tau_{1,B}, \tau_{2,A}, \tau_{2,B}\}}. \quad (12)$$

When l is sufficiently large, R approaches 1 symbol/channel.

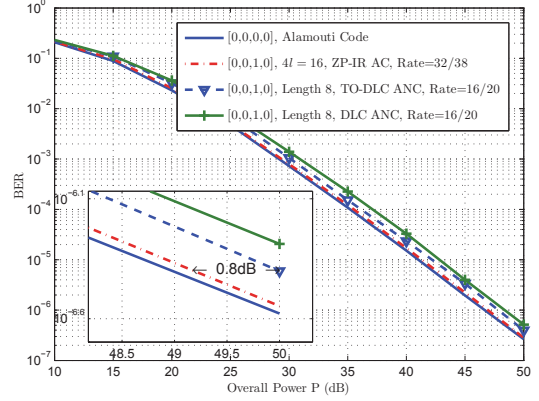


Fig. 5: Comparison of the BER performances of the Alamouti code [27], ZP-IR AC and ANC schemes [24](TO-DLC ANC and DLC ANC)

3.4. Fast ML Decoding

As Example 2 shows, the received signals \mathbf{y}_A can be decoupled into several independent parts to facilitate the ML decoding process. The complexity of the ML decoder at each terminal is $\mathcal{O}(4(l - 2\tau_m)|S| + 2\tau_m|S|^4)$, where $|S|$ is the cardinality of the constellation S .

4. SIMULATIONS

In this section, we present our simulation results on the performance of ZP-IR AC with the ML decoder. The channel fading coefficients follow an i.i.d. complex Gaussian distribution with zero-mean and unit variance. The maximum delay difference $\tau_m = 1$. Quadrature Phase Shift Keying (QPSK) is adopted in all the simulations.

Fig. 4 shows the bit error rate (BER) performance of ZP-IR AC with respect to the sum of all transmit power P , where the transmit power at each terminal is $P/4$. The performance of ZP-IR AC in delay profile $[0, 0, 0, 0]$ can be regarded as that of the Alamouti code [27] in the synchronized case. As can be seen, the performances of ZP-IR AC in the asynchronous cases are similar to that in the synchronized case. The diversity loss performance in Example 1 is also plotted. The difference in slope in the high overall power region represents the diversity gain difference.

Fig. 5 compares the BER performances of the synchronized Alamouti code [27], ZP-IR AC, and ANC schemes [24] (TO-DLC ANC and DLC ANC). The performance of ZP-IR AC is nearly the same as that of the synchronized Alamouti code. ZP-IR AC outperforms TO-DLC ANC and DLC ANC [24] with at least 0.8 dB. For sequence length, ANC schemes [24] have no requirement, while ZP-IR AC requires $4l \geq 8$ at least. For decoding complexity, when adopting large sequence length, ANC schemes [24] suffer from high complexity ML decoding, while ZP-IR AC does not. Therefore, for large sequence length, ZP-IR AC surpasses other codes because of its good BER performance and fast ML decoding.

5. CONCLUSION

This paper has proposed ZP-IR AC to achieve full diversity in an asynchronous two-way relay network. Through zero padding, ZP-IR AC achieves full diversity with fast ML decoding. Simulations showed the full diversity gain. Our work suggests that zero padding is an effective method to tackle symbol misalignment at the relays in two-way relay networks.

6. REFERENCES

- [1] S. Katti, S. Gollakota, and D. Katabi, "Embracing wireless interference: Analog network coding," in *Proceedings of the 2007 conference on Applications, technologies, architectures, and protocols for computer communications*, New York, NY, USA, 2007, SIGCOMM '07, pp. 397–408, ACM.
- [2] T. Cui, F. Gao, T. Ho, and A. Nallanathan, "Distributed space-time coding for two-way wireless relay networks," *IEEE Trans. on Signal Processing*, vol. 57, no. 2, pp. 658–671, 2009.
- [3] W. Wang, S. Jin, X. Gao, K.-K. Wong, and M.R. McKay, "Power allocation strategies for distributed space-time codes in two-way relay networks," *IEEE Trans. on Signal Processing*, vol. 58, no. 10, pp. 5331–5339, 2010.
- [4] S. J. Alabed, J. M. Paredes, and A. B. Gershman, "A simple distributed space-time coded strategy for two-way relay channels," *IEEE Trans. on Wireless Communications*, vol. 11, no. 4, pp. 1260–1265, 2012.
- [5] Q. Huo, L. Song, Y. Li, and B. Jiao, "A distributed differential space-time coding scheme with analog network coding in two-way relay networks," *IEEE Transactions on Signal Processing*, vol. 60, no. 9, pp. 4998–5004, 2012.
- [6] S. Zhang, S.-C. Liew, and P. P. Lam, "Physical-layer network coding," in *Proceedings of ACM Mobicom*, Sept 2006, pp. 358–365.
- [7] X. Li, "Space-time coded multi-transmission among distributed transmitters without perfect synchronization," *IEEE Signal Processing Letters*, vol. 11, no. 12, pp. 948–951, Dec. 2004.
- [8] S. Zhang, S.-C. Liew, and P. P. Lam, "On the synchronization of physical-layer network coding," in *IEEE Information Theory Workshop, 2006. ITW '06 Punta del Este.*, 2006, pp. 404–408.
- [9] Y. Mei, Y. Hua, A. Swami, and B. Daneshrad, "Combating synchronization errors in cooperative relays," in *IEEE International Conference on Acoustics, Speech, and Signal Processing, 2005. Proceedings. (ICASSP '05).*, March 2005, vol. 3, pp. 369–372.
- [10] L. Lu and S.-C. Liew, "Asynchronous physical-layer network coding," *IEEE Trans. on Wireless Communications*, vol. 11, no. 2, pp. 819–831, Feb. 2012.
- [11] S. Wei, D. L. Goekel, and M. C. Valenti, "Asynchronous cooperative diversity," *IEEE Trans. on Wireless Communications*, vol. 5, no. 6, pp. 1547–1557, June 2006.
- [12] Y. Shang and X.-G. Xia, "Shift-full-rank matrices and applications in space-time trellis codes for relay networks with asynchronous cooperative diversity," *IEEE Trans. on Information Theory*, vol. 52, no. 7, pp. 3153–3167, July 2006.
- [13] M. O. Damen and A. R. Hammons, "Delay-tolerant distributed-TAST codes for cooperative diversity," *IEEE Trans. on Information Theory*, vol. 53, no. 10, pp. 3755–3773, Oct. 2007.
- [14] Z. Li and X.-G. Xia, "A simple Alamouti space-time transmission scheme for asynchronous cooperative systems," *IEEE Signal Processing Letters*, vol. 14, no. 11, pp. 804–807, Nov. 2007.
- [15] Y. Li, W. Zhang, and X.-G. Xia, "Distributive high-rate space-frequency codes achieving full cooperative and multipath diversities for asynchronous cooperative communications," *IEEE Trans. on Vehicular Technology*, vol. 58, no. 1, pp. 207–217, Jan. 2009.
- [16] Z. Zhong, S. Zhu, and A. Nallanathan, "Delay-tolerant distributed linear convolutional space-time code with minimum memory length under frequency-selective channels," *IEEE Trans. on Wireless Communications*, vol. 8, no. 8, pp. 3944–3949, Aug. 2009.
- [17] N. Wu and H. Gharavi, "Asynchronous cooperative MIMO systems using a linear dispersion structure," *IEEE Trans. on Vehicular Technology*, vol. 59, no. 2, pp. 779–787, Feb. 2010.
- [18] M. R. Bhatnagar, A. Hjørungnes, and M. Debbah, "Delay-tolerant decode-and-forward based cooperative communication over Ricean channels," *IEEE Trans. on Wireless Communications*, vol. 9, no. 4, pp. 1277–1282, April 2010.
- [19] M. Sarkiss, G. R. B. Othman, M. O. Damen, and J. C. Belfiore, "Construction of new delay-tolerant space-time codes," *IEEE Trans. on Information Theory*, vol. 57, no. 6, pp. 3567–3581, June 2011.
- [20] W. Wang, F.-C. Zheng, A. Burr, and M. Fitch, "Design of delay-tolerant linear dispersion codes," *IEEE Trans. on Communications*, vol. 60, no. 9, pp. 2560–2570, Sept. 2012.
- [21] Y. Liu, W. Zhang, and P. C. Ching, "Full-diversity distributed space-time codes with an efficient ML decoder for asynchronous cooperative communication," in *IEEE International Conference on Acoustics, Speech, and Signal Processing, 2013. Proceedings. (ICASSP '13).*, May 2013.
- [22] Z. Li, X.-G. Xia, and B. Li, "Achieving full diversity and fast ml decoding via simple analog network coding for asynchronous two-way relay networks," *IEEE Trans. on Communications*, vol. 57, no. 12, pp. 3672–3681, Dec 2009.
- [23] Z. Fang, F. Liang, S. Zhang, and T. Peng, "A cyclic shift relaying scheme for asynchronous two-way relay networks," *Wireless Personal Communications*, vol. 71, no. 4, pp. 2863–2876, Aug 2013.
- [24] H.-M. Wang, X.-G. Xia, and Q. Yin, "A linear analog network coding for asynchronous two-way relay networks," *IEEE Trans. on Wireless Communications*, vol. 9, no. 12, pp. 3630–3637, Dec. 2010.
- [25] X. Guo and X.-G. Xia, "Distributed linear convolutional space-time codes for asynchronous cooperative communication networks," *IEEE Trans. on Wireless Communications*, vol. 7, no. 5, pp. 1857–1861, May 2008.
- [26] Y. Jing and H. Jafarkhani, "Using orthogonal and quasi-orthogonal designs in wireless relay networks," *IEEE Trans. on Information Theory*, vol. 53, no. 11, pp. 4106–4118, 2007.
- [27] S. M. Alamouti, "A simple transmit diversity technique for wireless communications," *IEEE Journal on Selected Areas in Communications*, vol. 16, no. 8, pp. 1451–1458, Oct. 1998.